Structure and dynamics of ferroelectric liquid crystal cells exhibiting thresholdless switching

Martin Čopič,[1,2] Joseph E. Maclennan,[2] and Noel A. Clark[2]
[1]*Department of Physics, University of Ljubljana, Jadranska 19, SI-1000 Ljubljana, Slovenia*
[2]*Ferroelectric Liquid Crystal Materials Research Center, Department of Physics, University of Colorado at Boulder, Boulder, Colorado 80309-0390*
(Received 5 July 2001; published 25 January 2002)

Surface-stabilized ferroelectric liquid crystal cells are usually bistable, with the spontaneous polarization either up or down, perpendicular to the plane of the cell. In materials with high spontaneous polarization the polarization charge self-interaction leads to a monostable structure that exhibits a thresholdless, ''V-shaped'' switching of the optical response to an applied voltage. With a model that includes the electrostatic self-energy of the spontaneous polarization, we examine the transition from bistablity to monostability as a function of the polar and nonpolar anchoring energies, the liquid crystal elasticity, and the thickness of the alignment layers. Two bistable and one monostable structures are possible. The bistable state is only obtained when the thickness of the insulating alignment layer and the polar anchoring energy are small, or when the spontaneous polarization is small. From linear stability analysis we get analytical expressions for the limits of stability of the structures. Numerical calculations show that in some ranges of the parameters two structures can coexist. We also present the calculation of the polarization fluctuation modes. The lowest one becomes soft at the continuous transitions among the structures and at the limits of stability.

DOI: 10.1103/PhysRevE.65.021708 PACS number(s): 61.30.Cz, 61.30.Gd, 42.79.Kr

I. INTRODUCTION

Chiral ferroelectric liquid crystals confined between parallel plates that induce planar alignment of the liquid crystal director can form structures with the smectic layers perpendicular to the cell plates (bookshelf geometry). When the cell thickness is smaller than the pitch of the SmC^* phase, the helix is suppressed and the director structure is the same in all layers—a surface-stabilized ferroelectric liquid crystal (SSFLC) is obtained. The most well known SSFLC structure is bistable [1]. In an ideal case, the spontaneous polarization **P** points in either direction (up or down) perpendicular to the plane of the cell and the optic axis is in the plane of the cell at one or the other extreme position on the SmC^* tilt cone, so that in switching from one stable state to the other the optic axis rotates by twice the cone angle. The transition from the up to the down state can be achieved by applying an external electric field.

In some planar-aligned and surface-stabilized cells of chiral smectic liquid crystals a different type of switching is obtained [2]. With crossed polarizer and analyzer perpendicular and parallel to the normal to smectic layers, the optical transmission curve is symmetric around zero voltage and is characteristically ''V shaped,'' that is, it rises nearly linearly until it reaches saturation at some voltage $\pm V_\varepsilon$. Since such cells always return to the same state at zero voltage, they are monostable. This means that the applied electric field induces continuous reorientation of the optic axis, which is along the layer normal for zero applied voltage, $V=0$. Recent experiments on ''V-shaped'' switching cells have demonstrated that the effect is a feature of the ferroelectric SmC^* phase [3], and that the rotation of the optic axis is due to the reorientation on the smectic C^* cone [3,4]. It has also been shown that the effect is electrostatic in origin [5], a result of the spontaneous polarization self-interaction, which becomes important in materials with sufficiently high P.

The mechanism can be understood in the following way. Consider a slab of SmC^* material in a bookshelf structure as depicted in Fig. 1. The cell is formed by two conducting electrodes separated from the liquid crystal by an insulating alignment layer. Let $V=0$ initially. The anchoring at the surface is planar, so that the minimum surface energy is obtained for **P** perpendicular to the surface. The perpendicular (x) component of **P** creates a surface polarization charge that must be compensated by free charges on the electrodes. Since these are separated from the liquid crystal by the alignment layer, an electric field is created in the alignment layer. When the electrostatic energy of this field is greater than the surface anchoring energy, it is energetically favorable for the polarization to orient parallel to the cell plates, breaking the surface anchoring. This situation is of course monostable. The importance of the field in the alignment layer was already recognized in Ref. [6]. As the electrostatic energy of

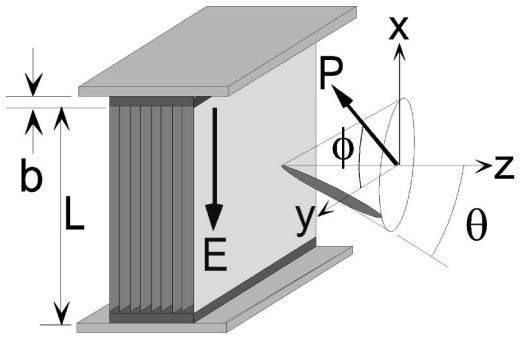

FIG. 1. Bookshelf geometry of a tilted chiral smectic. The liquid crystal is between glass plates with transparent ITO electrodes coated with nonconducting alignment layers. The smectic layers are normal to the plates. Shown are the tilt cone angle θ relative to the layer normal **z** the spontaneous polarization **P**, and the azimuthal orientation ϕ of **P**. ''V-shaped'' switching is observed with normally incident light between crossed polarizers.

the alignment layer is proportional to P^2, a monostable state is obtained for high P materials.

Thresholdless switching has also been attributed to antiferroelectricity in planar smectic liquid crystal cells [7]. Theoretical modeling of the effect in antiferroelectric liquid crystals has recently been presented in Refs. [8] and [9].

Both the bistable and monostable structures are very important for display applications. Their respective electrooptic characteristics are quite different, so it is important to understand what the parameters are that determine which structure is obtained. In this paper we present the results of model calculations of the director configurations obtained for different surface anchoring properties, spontaneous polarization, and elasticity of the liquid crystal. The stability of different structures and the nature of the transitions between them are closely associated with the lowest relaxation rate dynamic mode of the system, which we also calculate in our model. In the following, we first give some energy considerations showing which structures can occur, and then give detailed numerical results for the stability of the structures and the relaxation rate of the lowest polarization fluctuation mode as a function of the relevant parameters.

II. FREE ENERGY AND EQUILIBRIUM STRUCTURES

The equilibrium structures that can exist in SSFLC cells can be understood by examining the free energy of the system. The cell of thickness L, shown in Fig. 1, is formed by two conducting electrodes separated from the liquid crystal by insulating alignment layers of thickness $b \ll L$ and dielectric constant ε_1. The cell is assumed to be homogeneous in the plane of the plates, so that **P** depends only on the x coordinate and the electric field **E** only has an x component. The total energy of the cell is the sum of the elastic, electrostatic, and surface energies. The total field is $\sigma/(\varepsilon_1\varepsilon_0) - P\sin\phi$ in the liquid crystal, and $\sigma/(\varepsilon\varepsilon_0)$ in the alignment layer, where σ is free charge surface density on the electrodes. At constant σ the free energy of the system is

$$F=\int_{-L/2}^{L/2}\left[\frac{1}{2}K\left(\frac{d\phi}{dx}\right)^2+\frac{1}{2\varepsilon\varepsilon_0}P^2\sin^2\phi-\frac{\sigma}{\varepsilon\varepsilon_0}P\sin\phi\right]dx+\left(\frac{b}{\varepsilon_1\varepsilon_0}+\frac{L}{2\varepsilon\varepsilon_0}\right)\sigma^2+W_S, \tag{1}$$

where K is an effective elastic constant, ε the dielectric constant of the liquid crystal, and W_S the surface energy. The second term in the square brackets is the self-energy of the spontaneous polarization, and the third term describes the interaction of **P** with the field due to σ. The first term outside the integral is the electrostatic energy of the field due to σ in the liquid crystal and alignment layer. In Eq. (1) we have neglected the dependence of the liquid crystal dielectric tensor on ϕ, i.e., we have assumed a constant ε. As we have the voltage V between the electrodes that is fixed, not σ, we must transform Eq. (1) to free enthalpy $G=F-V\sigma$ and express σ in terms of V. Integrating the total field over the alignment layer and liquid crystal we have

$$V=\sigma\left(\frac{2b}{\varepsilon_1\varepsilon_0}+\frac{L}{\varepsilon\varepsilon_0}\right)-\frac{1}{\varepsilon\varepsilon_0}\int_{-L/2}^{L/2}P\sin\phi\,dx, \tag{2}$$

and

$$G=\int_{-L/2}^{L/2}\left[\frac{1}{2}K\left(\frac{d\phi}{dx}\right)^2+\frac{1}{2\varepsilon\varepsilon_0}P^2\sin^2\phi\right]dx-\frac{\varepsilon\varepsilon_0}{2L(1+a)}\times\left(V+\frac{1}{\varepsilon\varepsilon_0}\int_{-L/2}^{L/2}P\sin\phi dx\right)^2+W_S, \tag{3}$$

where we have introduced $a=2\varepsilon b/(\varepsilon_1 L)$ as the reduced thickness of the alignment layer.

The anchoring energy for **P** pointing into or out of the surface is usually not the same, and the surface anchoring energy can be decomposed into a nonpolar part invariant with respect to polarization reversal, and a polar part that depends on the polarity of **P** with respect to the normal to the surface. We write W_S in the form

$$W_S=-w_1[\sin\phi(-L/2)-\sin\phi(L/2)]-w_2[\sin^2\phi(-L/2)+\sin^2\phi(L/2)]. \tag{4}$$

The equilibrium structure of the system is obtained by minimizing G with respect to $\phi(x)$.

To see that more than one equilibrium structure can exist in an SSFLC cell, we first qualitatively examine different contributions to G. Let $V=0$, corresponding to a short-circuited cell. Spatial inhomogeneities of **P** produce polarization charges and an internal field in the liquid crystal, increasing the electrostatic energy. So in a material with high spontaneous polarization **P** will tend to be homogeneous in most of the liquid crystal slab. Let us first neglect the polar part of W_S, and assume that **P** and ϕ are constant. Then

$$G=\frac{b}{\varepsilon_1\varepsilon_0(1+a)}P^2\sin^2\phi-2w_2\sin^2\phi. \tag{5}$$

The first term is just the electrostatic energy of the alignment layer. When

$$P^2<2\varepsilon_1\varepsilon_0 w_2\frac{1+a}{b}, \tag{6}$$

the equilibrium state will be the one with polarization perpendicular to the slab, pointing either up or down. This is the usual bistable bookshelf structure and we designate it by B. For larger P, not satisfying Eq. (6), it is advantageous for the surface anchoring to break so that **P** is in the plane of the slab ($\phi=0$) and the electrostatic energy is zero. This structure exhibits monostable "V-shaped" switching, and we designate it by V. For the V state the field inside liquid crystal is zero. It remains zero even with an applied voltage $|V|<2bP/(\varepsilon_1\varepsilon_0)$ [5].

Consider now the effect of liquid crystal elasticity. Inspection of the first two terms of Eq. (1) shows that $\xi=\sqrt{\varepsilon\varepsilon_0 K/P^2}$ has the dimension of length. When ξ is much smaller than the sample thickness, it gives the thickness of deformed layers at the surfaces when the anchoring condi-

tions dictate different orientation of **P** than the electrostatic energy. ξ can be used as a measure of the liquid crystal elasticity. We first examine the stability of the B structure with respect to small perturbations from $\phi=\pi/2$, again setting the polar part of the anchoring $w_1=0$. Let us introduce $\psi=\pi/2-\phi$. The quadratic part of the free energy G in terms of ψ for $V=0$ is

$$G=\int_{-L/2}^{L/2}\left[\frac{1}{2}K\left(\frac{d\psi}{dx}\right)^2-\frac{a}{2\varepsilon\varepsilon_0(1+a)}P^2\psi^2\right]dx + w_2[\psi(-L/2)^2+\psi(L/2)^2]. \tag{7}$$

The function that makes G extremal is of the form $\psi=A\cos\kappa x$, with $\kappa=\sqrt{aP^2\varepsilon\varepsilon_0(1+a)K}$. Inserting it back in Eq. (7), we see that G has a minimum for a finite value of A when

$$w_2<\frac{P}{2}\left(\frac{aK}{\varepsilon\varepsilon_0(1+a)}\right)^{1/2}\tan\frac{\kappa L}{2}=\frac{P^2}{2\varepsilon\varepsilon_0}\frac{a}{(1+a)\kappa}\tan\frac{\kappa L}{2}. \tag{8}$$

For values of w_2 satisfying condition (8) the stable structure is inhomogeneous, with splayed spontaneous polarization, while for larger w_2 the B structure is stable. The actual value of A, giving the amount of splay, can of course only be obtained by keeping higher-order terms in G. The splayed structure is still bistable, as it can be either close to $\phi=\pi/2$ or $\phi=-\pi/2$, so we designate it by $B_{\rm def}$. For large elastic constant K, so that $\xi\gg L$ and $\kappa L\ll 1$, condition (8) reduces to the simple condition (6) for the stability of the B structure obtained above. For a less elastically stiff system the critical value of w_2 increases, that is, the range of stability of the B structure is decreased, from which we can infer that there exists a range of values of w_2 in which $B_{\rm def}$ is also stable with respect to the V structure. Condition (8) also shows that for $\kappa L>\pi$ the homogeneous B structure is never stable.

We note here that in Eqs. (6) and (8) and similar expressions below, the polarization energy density acts as a scaling factor. So for materials with smaller polarization the B structure is stable at smaller w_2. As w_2 is determined by the preparation procedure of the surface (the amount of rubbing, etc.), and does not depend on P, experimentally with small P one obtains the bistable B structure and with large P the monostable V structure.

The analysis of the stability of B towards $B_{\rm def}$ can easily be extended for $w_1\neq 0$. We find that B becomes unstable for

$$w_2<\frac{P}{2}\left(\frac{aK}{\varepsilon\varepsilon_0(1+a)}\right)^{1/2}\times\frac{\left(1+\frac{\varepsilon\varepsilon_0(1+a)w_1^2}{aKP^2}\sin^2\kappa D\right)^{1/2}-\cos\kappa L}{2\sin\kappa L}, \tag{9}$$

which shows that increasing the polar part (w_1) of the anchoring energy also reduces the stability of the pure bookshelf structure B.

The stability of the V structure can be analyzed in a similar way. We assume that ϕ is small throughout the slab and again take only the quadratic part of G with $V=0$,

$$G=\int_{-L/2}^{L/2}\left[\frac{1}{2}K\left(\frac{d\phi}{dx}\right)^2+\frac{1}{2\varepsilon\varepsilon_0}P^2\phi^2\right]dx - \frac{P^2}{2\varepsilon\varepsilon_0 L(1+a)}\left(\int_{-L/2}^{L/2}\phi\,dx\right)^2+Ws, \tag{10}$$

where $W_S=-w_1[\phi(-L/2)-\phi(L/2)]-w_2[\phi(-L/2)^2+\phi(L/2)^2]$. In order that ϕ be small at the boundaries, K must not be too small with respect to w_1. We now get an inhomogeneous Euler-Lagrange equation

$$-\xi^2\frac{d^2\phi}{dx^2}+\phi=\frac{1}{(1+a)L}\int_{-L/2}^{L/2}\phi\,dx, \tag{11}$$

with the solution $\phi=A\sinh(x/\xi)+B[\cosh(x/\xi)+(2\xi/aL)\sinh(L/2\xi)]$, where A and B are constants. Inserting this solution back into expression (10) and requiring that G is minimal we get

$$A=\frac{w_1}{\sqrt{KP^2/\varepsilon\varepsilon_0}\cosh L/2\xi-2w_2\sinh L/2\xi} \tag{12}$$

and find that $B\neq 0$ if

$$w_2>\frac{bP^2}{\varepsilon_1\varepsilon_0}\frac{\sinh L/2\xi}{2\sinh L/2\xi+a/\xi\cosh L/2\xi}. \tag{13}$$

When $B=0$ we have the V structure with a deformed boundary layer due to finite w_1 and K. The divergence of A for w_2 large enough, so that the denominator of Eq. (12) becomes zero, has no direct physical meaning because the linear approximation is not valid for large A, but we will see later in the numerical results that we indeed get some new interesting features for large w_2. Nonzero value of B represents the $B_{\rm def}$ structure. For an elastically stiff system, where ξ is large, condition (13) again reduces to the simple condition (6) for the B to V transition. In the limit of small ξ, the transition from V to $B_{\rm def}$ occurs at $w_2=P^2a\xi/2\varepsilon\varepsilon_0=Pa\sqrt{K/4\varepsilon\varepsilon_0}$.

Let us look at a specific material like W415 [10], taking $P=300\,{\rm nC/cm^2}$, $\varepsilon=10$, and $L=2\,\mu{\rm m}$. A realistic value for the thickness of the alignment layer in typical cells is $b=10\,{\rm nm}$ and for its dielectric constant $\varepsilon_1=10$. We then get that $a=0.01$ and $\xi/L=0.005$, so that we are in the above limit of small ξ. The V structure will be stable for nonpolar anchoring energy $w_2<2\times10^{-4}\,{\rm J/m^2}$, which represents a relatively strong anchoring. We also get that $\kappa L=20$, which is much larger than π, so that the pure B structure is never stable. If the spontaneous polarization is 10 times smaller, the transition from V to $B_{\rm def}$ occurs at $w_2\approx2\times10^{-5}\,{\rm J/m^2}$. This is smaller than usual anchoring energies of well prepared samples, so in low P materials, bistable switching is usually observed. According to Eq. (8) we now also get the transition from $B_{\rm def}$ to B with $w_1=0$ at $w_2=10^{-4}\,{\rm J/m^2}$,

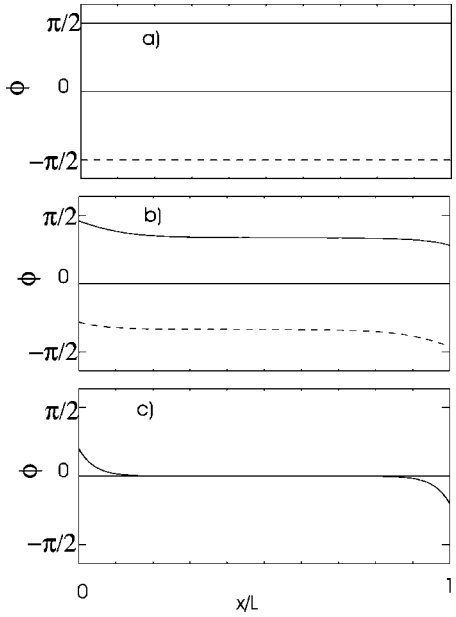

FIG. 2. Polarization angle ϕ as a function of position for the three possible structures. (a) The B structure is homogeneous and bistable with $\phi=\pm\pi/2$. (b) In the B_{def} structure there is a deformed layer of thickness $\xi=\sqrt{P^2/\varepsilon\varepsilon_0 K}$ at each surface, and in the middle of the cell $0<|\phi|<\pi/2$, so the structure is also bistable. (c) In the monostable V structure there is a deformed surface layer of thickness ξ and in the middle of the cell $\phi=0$.

while with $w_1=10^{-4}\,\mathrm{J/m^2}$, the transition value of w_2, according to Eq. (9), increases by about 20%.

Figure 2 shows all the possible structures obtained by the stability analysis of the free enthalpy functional. For large nonpolar anchoring energy w_2, thin insulating alignment layer, and large $\xi=\sqrt{\varepsilon\varepsilon_0 K/P^2}$, the pure bookshelf structure B is stable [Fig. 2(a)]. By decreasing w_2 first the deformed bistable structure B_{def} [Fig. 2(b)], then the monostable V structure, characterized by the ''V-shaped'' switching is obtained [Fig. 2(c)]. For small ξ the B structure is never stable, while for large ξ, the B_{def} structure disappears. Figure 2(b) and 2(c) assume a nonzero w_1. For $w_1=0$, the B_{def} structure is even with respect to the center of the cell, and the V structure has $\phi=0$ throughout.

III. NUMERICAL CALCULATION OF THE STABILITY DIAGRAMS

To get a more detailed picture of the stable structures and the transitions among them, we must consider the complete expression for the free enthalpy G and find its minima numerically. We divide the cell thickness (x axis) into n intervals, where n is usually 100, and take L as the unit of length. We also introduce the dimensionless free enthalpy $g=\varepsilon\varepsilon_0 G/LP^2$, a relative stiffness parameter $k=\xi^2/L^2$, dimensionless anchoring strengths r_1 and r_2 with $r_i=\varepsilon\varepsilon_0 w_i/LP^2$, and the dimensionless voltage $v=\varepsilon\varepsilon_0 V/LP$. With this choice of the dimensionless parameters the magnitude of P acts as a scaling parameter. k and r_2 scale as $1/P^2$. The polar anchoring strength w_1 depends generally on both steric and dipolar interactions between the surface and the liquid crystal molecules, so w_1 probably has a less than linear dependence on P, but we still expect it to increase with increasing P. Then r_1 should scale as $P^{-\alpha}$, with α between 1 and 2. As the spontaneous polarization is temperature dependent, some of the features of the stability of the structures with respect to the values of the parameters, discussed below, could be experimentally observable by analyzing the structure of a given sample as a function of temperature.

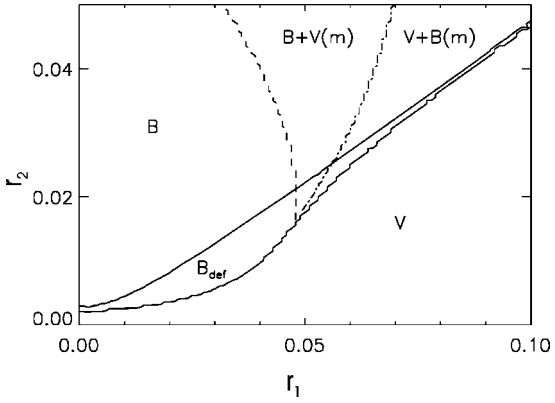

FIG. 3. Stability diagram of the structures vs the polar and nonpolar anchoring parameters r_1 and r_2 ($r_1=\varepsilon\varepsilon_0 w_i/LP^2$) for the scaled alignment layer thickness $a=0.01$ and stiffness $k=\xi^2/L^2=0.01$. $\mathsf{V}(m)$ and $B(m)$ designate metastable structures. Solid curves indicate continuous transitions between structures. The dashed curve is the limit of stability of the $\mathsf{V}(m)$ structure, and the dot-dashed curve shows where the free enthalpies of V and B are equal.

We use the trapezoidal rule for integration, so that

$$g=\frac{1}{2n}\sum_{i=1}^{n}\left[k(\phi_i-\phi_{i-1})^2n^2+\sin^2\phi_i\right]-\frac{1}{4n}(\sin^2\phi_0+\sin^2 gf_n)-\frac{1}{2(1+a)}\left[v+\frac{1}{n}\sum\sin\phi_i-\frac{1}{2n}(\sin\phi_0+\sin\phi_n)\right]^2-r_1(\sin\phi_0-\sin\phi_n)-r_2(\sin^2\phi_0+\sin^2\phi_n). \tag{14}$$

The additional endpoint terms come from the trapezoidal integration formula and can significantly affect the results for small anchoring energies. We minimize g with respect to the values ϕ_i using the Davidon-Fletcher-Powell method [11]. In order not to miss any metastable structures, we do two minimizations for every choice of the values of the parameters, once starting with values for ϕ_i close to 0 and once close to $\pi/2$.

Figure 3 shows the stability diagram with respect to the two anchoring parameters r_1 and r_2 for a moderate value of the stiffness parameter k. As expected, the V structure is stable for small nonpolar anchoring r_2, while for large r_2 the B structure is stable. Larger values of polar anchoring in-

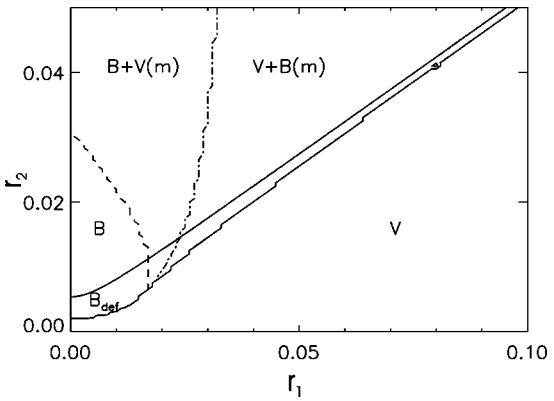

FIG. 4. Same as in Fig. 3, with smaller stiffness $k=\xi^2/L^2=0.0016$.

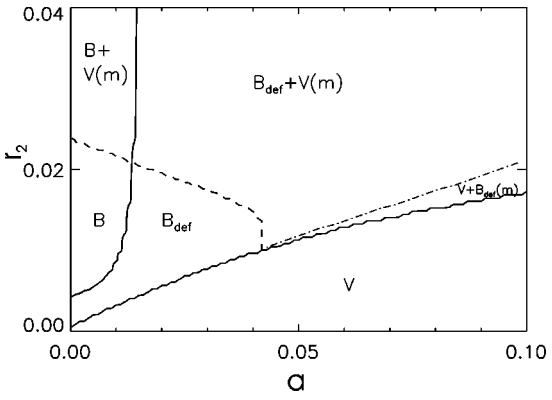

FIG. 5. Stability diagram of the structures vs the scaled alignment layer thickness a and the nonpolar anchoring parameters $r_2=\varepsilon\varepsilon_0 w_2/LP^2$, for $r_1=0.01$ and stiffness $k=\xi^2/L^2=0.0016$. V(m) and $B(m)$ designate metastable structures. Solid curves indicate continuous transitions between structures, dashed curve is the limit of stability of the V(m) structure, and the dot-dashed curve shows where the free enthalpies are equal. For $a>0.015$ the homogeneous bookshelf B structure is unstable for all values of r_2.

crease the range of stability of the V structure. Between the V and B structures we get the $B_{\rm def}$ structure if r_1 is not too large.

The analytical results of the preceding section agree quite well with the numerical results. The numerically obtained transition line from the B to the $B_{\rm def}$ structure is the same as calculated by Eq. (9), while the transition to the V structure at small r_1 is accurately given by Eq. (13).

There are also some new features not obtained by the linear stability analysis. For small and moderate values of r_1 the transitions are continuous, but for $r_1>0.05$ (in the upper right part of Fig. 3) two structures can coexist: we can either have a stable V structure and a metastable V structure, or a stable V and metastable B structure. It is very interesting that the limit of metastability of the V-structure curves back towards smaller values of r_1 with increasing r_2, so that the metastable V structure is reentrant at large r_2. This is understandable intuitively: large r_2 means a large potential barrier at $\phi=0$ and since r_1 causes a deformed surface layer, this potential barrier pins the polarization at the symmetric midposition. Likewise in the case of the metastable B structure going into V structure, ϕ at one surface must climb over the potential barrier at $\phi=0$. In Fig. 3 the line separating the regions of metastibility of the two structures is determined by examining where the free enthalpies of the two structures are equal.

Figure 4 shows the stability diagram vs r_1 and r_2 for a smaller value of the stiffness parameter k. The general features of Fig. 3 are retained except that the coexistence region is considerably increased. This is to be expected as smaller k means larger (and narrower) deformations at the boundaries and, therefore, a more pronounced effect of the surface energy barrier at $\phi=0$. Also not surprisingly, at smaller r_1 the stability of the $B_{\rm def}$ structure, as evidenced by the relative size of the interval of r_2 in which it exists, is increased.

The stability diagram vs the effective thickness of the alignment layer a and nonpolar anchoring parameter r_2 is shown in Fig. 5. At small r_1 we again get a domain of stable V structure, the width of which increases with increasing a. At small a and large r_2 we get the B structure. For thicker alignment layers and large r_2 we get the $B_{\rm def}$ structure. It is interesting that for sufficiently large a the B structure does not appear for any value of r_2. This is understandable: for large a the electrostatic energy of the alignment layer in the B structure is larger than the energy of the deformed layer with $\phi=\pi/2$ at the surface in the $B_{\rm def}$ structure, so that increasing r_2 has no effect. At larger values of r_2 we again get coexisting structures, with the V structure stable and the $B_{\rm def}$ structure metastable in the middle domain on the right, and $B_{\rm def}$ or B stable and V metastable in the upper part of Fig. 5.

For k close to 1, a rather large value of the stiffness parameter that would occur in a material with a small $P \lesssim 3\ {\rm nC/cm^2}$, the stability diagram becomes much simpler. The $B_{\rm def}$ structure disappears and we have the B structure for reasonable values of r_2. For small r_2, that is for w_2 of the order of 10^{-6}–$10^{-7}\ {\rm J/m^2}$, we get a direct transition to the V structure with increasing either a or r_1. As $w_2=10^{-6}\ {\rm J/m^2}$ is an unrealistically small value, the B structure, possibly accompanied by a chevron, is generally observed in low P materials.

IV. FLUCTUATIONS

The dynamics of the system can be most conveniently obtained through Landau-Khalatnikov formalism. Assuming a single viscosity η, the rate of relaxation of ϕ towards equilibrium is given by

$$\eta\frac{\partial\phi}{\partial t}=\frac{\delta G}{\delta\phi}. \tag{15}$$

To get the small amplitude polarization fluctuation modes and their relaxation rates we have to linearize Eq. (15) around the equilibrium configuration and solve the resulting eigenfunction and eigenvalue problem. As we only have numerical solutions for the equilibrium configuration, this has to be done numerically too. An equivalent procedure for low order modes with wave numbers much smaller than $1/\Delta x$,

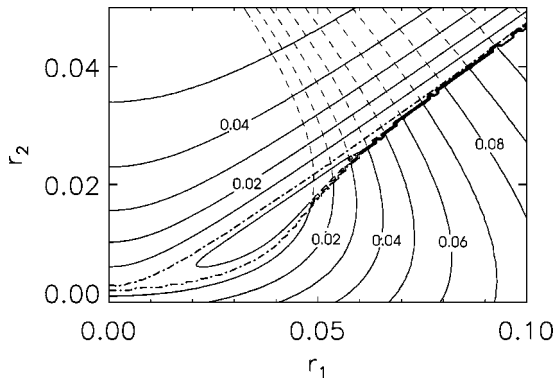

FIG. 6. Contour plot of the fundamental mode relaxation rate vs the polar and nonpolar anchoring parameters r_1 and r_2 ($r_i = \varepsilon\varepsilon_0 w_i / LP^2$) for alignment layer thickness $a=0.01$ and stiffness $k=\xi^2/L^2=0.01$ (compare with Fig. 3.). The mode relaxation rate goes to zero at the continuous transition lines (dot dashed) and at the limit of stability of the V structure (end of dashed lines). The contour lines for the V structure in the region of coexistence with the *B* structure are shown dashed.

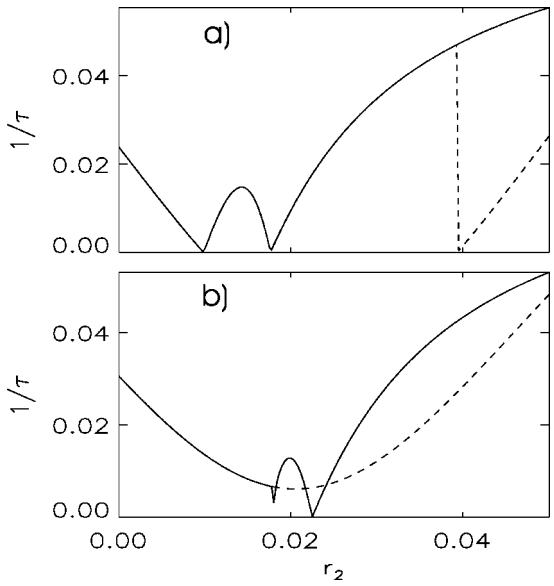

FIG. 7. Fundamental mode relaxation rate $1/\tau$ vs r_2 for two values of $r_1=0.04$ and $r_1=0.05$, with alignment layer thickness $a=0.01$ and stiffness $k=\xi^2/L^2=0.01$ (cuts through Fig. 6). In the region of the coexisting V and *B* structures the relaxation rate of the V structure is dashed. $1/\tau$ goes to zero at the continuous transitions (from both sides) and at the stability limits (from one side only).

where Δx is the size of the grid, is to form the matrix of the second derivatives of the free enthalpy, i.e., the susceptibility matrix

$$M_{ij}=\frac{\partial^2 g}{\partial\phi_i\partial\phi_j}. \tag{16}$$

The eigenvalues of this matrix, evaluated at a given equilibrium structure, are proportional to the relaxation rates of the polarization modes, with some effective viscosity as the proportionality factor. The shape of the modes can be obtained from the eigenvectors of **M**. Of course, in our model only the modes in the *x* direction are considered, as we do not allow spatial variations in the *y* and *z* directions. In a full three-dimensional treatment each mode would be a branch of fluctuations with continuous quadratic dependence of the relaxation rate on q_y and q_z.

The mode belonging to the lowest eigenvalue of **M** would be just the Goldstone (phase) mode in an infinite sample. Finite size and surface anchoring make the relaxation rate finite and strongly dependent on the thickness of the sample. This mode gives the dominant contribution to the dielectric response at low frequencies. It was first studied in Ref. [12], and has been called the ''thickness mode'' in Ref. [13].

The analysis of the slowest mode also shows very clearly the nature of the transitions among different structures. When a transition between two structures is continuous, the lowest relaxation rate goes to zero at the same point in control parameter space for both structures. In the case of coexisting structures, the lowest relaxation rate of each structure goes to zero at the limit of (meta)stability of the structure.

Figure 6 shows a contour plot of the lowest eigenvalue of **M** for stable or metastable structures as a function of r_1 and r_2, with the other parameters being the same as in Fig. 3. For clarity, in Fig. 7 we also present two cuts through Fig. 6 at constant r_1. For $r_1 \lesssim 0.03$, we have no coexisting structures, so the transitions from the *V* to $B_{\rm def}$ and from the $B_{\rm def}$ to *B* structure are continuous and the relaxation rate goes to zero at the transition lines from both sides. At $r_1 \cong 0.04$, the transitions to the $B_{\rm def}$ and *B* structures are still continuous, with corresponding soft modes, but we also get the reentrant metastable V structure. At the limit of metastability of this structure, the relaxation rate of its lowest fluctuation mode (dashed line in Fig. 7) goes to zero, as expected. For larger values of r_1, for instance, $r_1=0.05$, the fundamental mode of the V structure never becomes soft, indicating that the *V* structure remains stable or metastable for all values of r_2. At large enough values of r_2, the $B_{\rm def}$ structure also becomes possible and goes to the *B* structure at a larger value of r_2. The corresponding relaxation rate starts from zero at the limit of metastability of the $B_{\rm def}$ structure and is again soft at the continuous transition to the *B* structure.

The fundamental fluctuation modes of the three structures are observable by dielectric spectroscopy or optically by light scattering. By examining the displacement of each mode we see that the dielectric strength of the mode is large in the V structure and at the *V* to $B_{\rm def}$ transition, and weak at the $B_{\rm def}$ to *B* transition. By light scattering the mode is always observable by a proper choice of the scattering geometry.

Figure 8 is a contour plot of the fundamental mode relaxation rate vs *a* and r_2. We again see the same features as in Fig. 6 and 7. At the continuous transition lines from *V* to $B_{\rm def}$ and from $B_{\rm def}$ to *B* the mode becomes soft. The relaxation rate of the structures also goes to zero at the limits of metastability of both the V and *B* structure.

V. APPLIED VOLTAGE RESPONSE

Our model also allows us to simulate the quasistatic response of the system to an applied voltage. The rate of

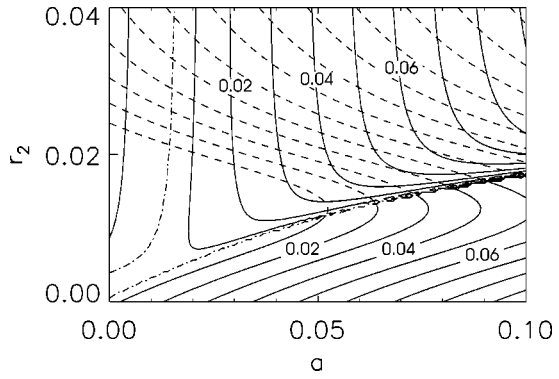

FIG. 8. Contour plot of the fundamental mode relaxation rate vs a and nonpolar anchoring parameter $r_2=\varepsilon\varepsilon_0 w_2/LP^2$ for $r_1=0.01$ and stiffness $k=\xi^2/L^2=0.01$ (compare with Fig. 5). The mode relaxation rate goes to zero at the continuous transition lines (dot-dashed) and at the limits of stability (end of dashed lines for the V structure and end of the contour lines for $B_{\rm def}$ structure for $a>0.04$). The contour lines for the V structure in the region of coexistence with the B structure are shown dashed.

change of the field must be small so that the viscous effects in switching are negligible. In practice this would mean that the frequency of the switching voltage should be smaller than a few hertz.

Figure 9 shows the polarization angle ϕ in the middle of the cell as a function of the applied voltage for three values of r_2 chosen so that at zero voltage the system is respectively in the V, $B_{\rm def}$, or B structures. At high enough voltage the system will always be homogeneous, with polarization parallel to the external field, $\phi=\pi/2$.

In the V structure, as the voltage is decreased from the maximum value, ϕ starts to decrease at some critical voltage V_c. The curve has a characteristic sigmoid shape, showing an approximately linear dependence on V around $V=0$. With polarizer and analyzer parallel and perpendicular to the smectic layer normal one would obtain the characteristic ''V-shaped'' optical response. The response of the $B_{\rm def}$-structure shows first some gradual elastic decrease, then a jump very close to $V=0$, as we would expect due to the bistable nature of the $B_{\rm def}$ structure, and finally an elastic approach to homogeneous state. But there is very little hysteresis in the response (the jump occurs very close to $V=0$). The response of the B structure has a jump at a voltage that is substantially negative, so it shows a large hysteresis. It also shows some initial elastic response before jumping to the other side of the SmC cone.

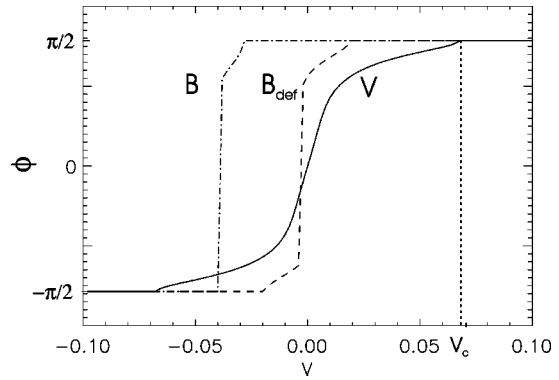

FIG. 9. Polarization angle in the middle of the cell vs applied voltage going from the positive to the negative side. The initial positive voltage is always such that the structure is homogeneous with $\phi=\pi/2$. The B structure shows a pronounced hysteresis. With no applied voltage, the systems considered here have respectively the V structure (solid line), the $B_{\rm def}$ structure (dashed line), and the B structure (dot-dashed line).

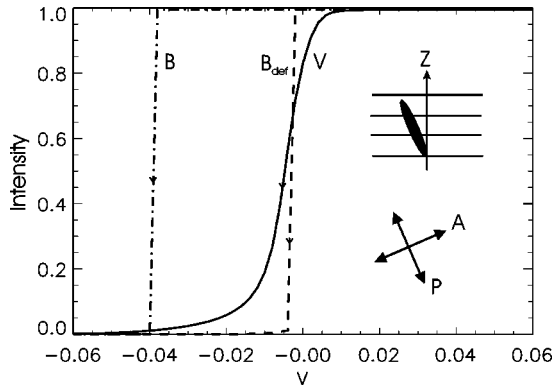

FIG. 10. Optical response vs applied voltage going from the positive to the negative side. The cell is between crossed polarizers aligned with the optic axis at the final negative voltage (inset), which is always such that the structure is homogeneous with $\phi=\pi/2$. Cell thickness corresponds to half-wave plate at the initial and final voltage. The B structure shows a pronounced hysteresis. With no applied voltage, the systems considered here have respectively the V structure (solid line), the $B_{\rm def}$ structure (dashed line), and the B structure (dot-dashed line).

In Fig. 10 we present the optical transmission of the cell vs applied voltage for the same values of the parameters as in Fig. 9. The thickness of the cell is such that it acts as a half-wave plate in a large applied voltage, that is, when the director is oriented uniformly on one side of the smectic cone. We take the cone angle $\theta=22.5°$, so that with crossed polarizers aligned with the optic axis when the voltage is at the maximum positive value, the transmission is maximum, and for maximum negative voltage the transmission is zero. The initial and final small deformations from the homogeneous state are nearly unobservable and the main change in the optical response occurs when ϕ reorients through 0. So for the V structure we get a rather linear response characteristic of ''V-shaped'' switching, while for the B and $B_{\rm def}$ structures we get a sharp step. In the $B_{\rm def}$ structure the step occurs very close to $V=0$. In experiments on switching at moderate frequencies, the viscous drag will change the step to a linear dependence on voltage which may be difficult to distinguish from the true ''V-shaped'' response.

It is also interesting to look at the fundamental mode relaxation rate as a function of the applied voltage, shown in Fig. 11. The behavior of the same three zero-field structures as in Figs. 9 and 10 is presented. For the values of parameters giving the V structure at zero field, in decreasing the voltage from the maximum positive value we first see a complete softening of the relaxation rate at some voltage V_c, where the transition from the homogeneous to the deformed

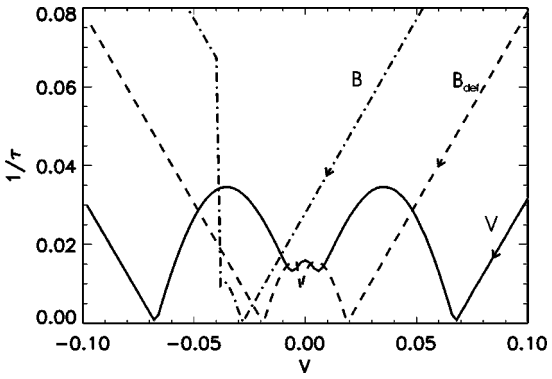

FIG. 11. Fundamental mode relaxation rate vs applied voltage going from the positive to the negative side. The initial positive voltage is always such that the structure is homogeneous with $\phi = \pi/2$. With no applied voltage, the systems considered here have respectively the V structure (solid line), the B_{def} structure (dashed line), and the B structure (dot-dashed line).

structure occurs. At any finite voltage the symmetry of the V structure is broken, and the V and B_{def} structures are indistinguishable so that no other sharp transition occurs, but we still get additional partial softening of the relaxation rate at small positive and negative voltage. The amount of softening depends on r_2 and becomes more pronounced close to the zero-field V-to-B_{def} transition.

The relaxation rate of the B_{def} structure also shows complete softening at the transition to the deformed structure. It completely softens again at a small negative voltage just before the structure jumps to the other side of the smectic cone. On the negative side of the jump the relaxation rate also goes discontinuously to a finite value. Then we again obtain a complete softening at the transition to the homogeneous structure.

For the B structure the first complete slowing down of the relaxation rate occurs well on the negative side of $V=0$, where the structure starts to deform elastically. The relaxation rate goes to zero again just before the system transforms to the homogeneous structure on the opposite side of the smectic cone, where the relaxation rate also jumps to a large value.

The behavior of the fundamental mode relaxation rate, as measured by dielectric spectroscopy and/or light scattering, as a function of temperature and applied voltage could be used to obtain some of the parameters of the system. Changing the temperature changes the magnitude of the spontaneous polarization, which in our model rescales the parameters r_1, r_2, and k. The main difficulty in analyzing measurements as a function of the applied voltage would come from the effect of internal field screening due to the free ions in the liquid crystal [14].

VI. CONCLUSIONS

We have presented model calculations of the structure and fluctuation dynamics of planar bookshelf ferroelectric liquid crystal cells including the electrostatic energy of the spontaneous polarization and the insulating alignment layer, the polar and nonpolar parts of the surface anchoring energy, and the elastic energy. Three structures are possible: homogeneous bistable (B), deformed bistable (B_{def}), and monostable "V switching" (V). The V structure is favored by high spontaneous polarization, thick alignment layers, and a large polar anchoring energy. When both the nonpolar and polar parts of the anchoring energy are large, the B and V structures can coexist and the transition between them is discontinuous. We have also shown that the relaxation rate of the fundamental polarization mode of the system behaves as the soft mode of the transitions between the structures. Its dependence on applied voltage and temperature should give valuable information on the parameters of the system.

In a broader context, our results also show that changes in textures of liquid crystals with polar smectic layers need not be due to a thermodynamic phase change. The structure of the domains in a liquid crystal texture can also change because the relative magnitudes of the electrostatic, elastic and surface energies vary, as presented in this paper. In addition, stable and metastable structures can coexist. This could perhaps help to explain the bewildering richness of the textures observed in the banana type sinectic phases.

ACKNOWLEDGMENTS

This work was supported by NSF MRSEC Grant No. DMR 98-09555 and ARO Grant No. DAAG 55-98-10446.

[1] N. A. Clark and S. T. Lagerwall, Appl. Phys. Lett. **36**, 899 (1980).

[2] S. Inui, N. Iimura, T. Suzuki, H. Iwane, K. Miyachi, Y. Takanishi, and A. Fukuda, J. Mater. Chem. **6**, 671 (1996); S. S. Seomun, B. Park, A. D. L. Chadani, D. S. Hermann, Y. Takanishi, K. Ishikawa, H. Takezoe, and A. Fukuda, Jpn. J. Appl. Phys., Part 2 **37**, L691 (1998); A. Fukuda, Y. Takanishi, K. Ishikawa, and H. Takezoe, J. Mater. Chem. **4**, 997 (1994).

[3] N. A. Clark, J. E. Maclennan, R. Shao, D. Coleman, S. Bardon, T. Bellini, D. R. Link, G. Natale, M. A. Glaser, D. M. Walba, M. D. Wand, X. H. Chen, P. Rudquist, J. P. F. Lagerwall, M. Buivydas, F. Gouda, and S. T. Lagerwall, J. Mater. Chem. **9**, 1257 (1999).

[4] B. Park, S. Seomun, M. Nakata, M. Takahashi, Y. Takanishi, and H. Takezoe, Jpn. J. Appl. Phys., Part 1 **38**, 1474 (1999).

[5] N. A. Clark, D. Coleman, and J. E. Maclennan, Liq. Cryst. **27**, 985 (2000).

[6] K. H. Yang, T. C. Chieu, and S. Osofsky, Appl. Phys. Lett. **55**, 125 (1989).

[7] S. Inui, N. Imura, T. Suzuki, H. Iwane, K. Miyachi, Y. Takanishi, and A. Fukuda, J. Mater. Chem. **6**, 671 (1996).

[8] N. J. Mottram and S. J. Elston, Liq. Cryst. **26**, 1853 (1999).

[9] N. J. Mottram and S. J. Elston, Phys. Rev. E **62**, 6787 (2000).

[10] R. F. Shao, J. E. Maclennan, N. A. Clark, D. J. Dyer, and D. M. Walba, Liq. Cryst. **28**, 117 (2001).

[11] W. H. Press, S. A. Teukolsky, W. T. Wetterling, and B. P. Flannery, *Numerical Recipes in C*, 2nd ed. (Cambridge University Press, Cambridge, 1992).

[12] Yu. P. Panarin, Yu. P. Kalmykov, S. T. MacLughadha, H. Xu, and J. K. Vij, Phys. Rev. E **50**, 4763 (1994).

[13] M. Glogarova, H. Sverenyak, J. Holakovsky, H. T. Nguyen, and C. Destrade, Mol. Cryst. Liq. Cryst. Suppl. Ser. **263**, 245 (1995).

[14] M. Čopič, J. E. Maclennan, and N. A. Clark, Phys. Rev. E **63**, 031703 (2001).